Phase Equilibria and Modeling of Pyridinium-Based Ionic Liquid Solutions

Urszula Domańska,[*,†,‡] **Marek Królikowski,**[†] **Deresh Ramjugernath,**[‡] **Trevor M. Letcher,**[‡] **and Kaniki Tumba**[‡,§]

Department of Physical Chemistry, Faculty of Chemistry, Warsaw University of Technology, Noakowskiego 3, 00-664 Warsaw, Poland, and Thermodynamic Research Unit, School of Chemical Engineering, University of KwaZulu-Natal, Howard College Campus, King George V Avenue, Durban 4001, South Africa

The phase diagrams of the ionic liquid (IL) *N*-butyl-4-methylpyridinium bis{(trifluoromethyl)sulfonyl}imide ([BM⁴Py][NTf₂]) with water, an alcohol (1-butanol, 1-hexanol, 1-octanol, 1-decanol), an aromatic hydrocarbon (benzene, toluene, ethylbenzene, *n*-propylbenzene), an alkane (*n*-hexane, *n*-heptane, *n*-octane), or cyclohexane have been measured at atmospheric pressure using a dynamic method. This work includes the characterization of the synthesized compound by water content and also by differential scanning calorimetry. Phase diagrams for the binary systems of [BM⁴Py][NTf₂] with all solvents reveal eutectic systems with regards to (solid−liquid) phase equilibria and show immiscibility in the liquid phase region with an upper critical solution temperature (UCST) in most of the mixtures. The phase equilibria (solid, or liquid−liquid) for the binary systems containing aliphatic hydrocarbons reported here exhibit the lowest solubility and the highest immiscibility gap, a trend which has been observed for all ILs. The reduction of experimental data has been carried out using the nonrandom two-liquid (NRTL) correlation equation. The phase diagrams reported here have been compared with analogous phase diagrams reported previously for systems containing the IL *N*-butyl-4-methylpyridinium tosylate and other pyridinium-based ILs. The influence of the anion of the IL on the phase behavior has been discussed.

Introduction

Pyridinium-based ionic liquids (ILs) because of their interesting properties are driving new research in many fields. In the past decade, much attention has been paid to the desulfurization of fuels.[1–4] Recently, our group determined the solubility of thiophene in ILs involving a pyridinium cation and tosylate or bis{(trifluoromethyl)sulfonyl}imide anion: *N*-butyl-4-methylpyridinium tosylate [BM⁴Py][TOS], *N*-butyl-3-methylpyridinium tosylate [BM³Py][TOS], *N*-hexyl-3-methylpyridinium tosylate [HM³Py][TOS], *N*-butyl-4-methylpyridinium bis{(trifluoromethyl)-sulfonyl}imide [BM⁴Py][NTf₂], 1,4-dimethylpyridinium tosylate [M¹,⁴Py][TOS], or 2,4,6-collidine tosylate [M²,⁴,⁶Py][TOS] at ambient pressure.[3] The specific properties of a broad liquidus temperature range, air and moisture stability, and solubility make pyridinium-based ILs potentially useful in different separation processes.[5–10] These ILs have been shown to have potentially excellent entrainer properties for the separation of aliphatic hydrocarbons from aromatic hydrocarbons by extractive distillation or extraction: pyridinium ethoxyethylsulfate [Py][C₂H₅O-C₂H₄SO₄],[5] *N*-ethyl-pyridinium bis{(trifluomethyl)sulfonyl}imide [EPy][NTf₂],[5] *N*-butyl-4-methylpyridinium tetrafluoroborate [BM⁴Py][BF₄],[6–9] and [MB⁴Py][NTf₂].[10] Butyl substitution is optimal for the selectivity of the separation aliphatics or aromatics because the separation decreases with an increasing length of the alkyl chain on the pyridinium cation of the IL.

Knowledge of the phase equilibria (solid−liquid equilibria, SLE, and liquid−liquid equilibria, LLE) in binary and ternary systems is important if ILs are to be considered as solvents in extraction processes.[3,4,11–13] Our recent work with [BM⁴Py][TOS]

and [BM³Py][TOS] has shown a high solubility of aromatic hydrocarbons and very small solubility of aliphatic hydrocarbons in these ILs.[12,13] Thus, they have the potential to be good solvents for separating organic liquids using solvent extraction or extractive distillation processes. It is, however, the thermodynamic information, which reflects how the different ILs interact with different solvents, that is crucial in assessing their usefulness and allows one to predict better and more efficient ILs. It has been shown that the IL composed of the [BM⁴Py]⁺ cation and an aromatic-based anion, such as the tosylate anion [TOS]⁻¹ (increasing the solubility of aromatic solvents in the IL), can be an effective solvent for the separation of aliphatic hydrocarbons from aromatic hydrocarbons.[14] However, the tosylate anion increases the melting temperature of the IL. An exchange of the IL's anion, from tosylate to bis{(trifluoromethyl)sulfonyl}imide, decreases the melting temperature of the IL and changes the solubility of the IL in water, alcohols, aromatic hydrocarbons, and thiophene.[3,11–13,15]

The information coming from the measurements of the activity coefficients at infinite dilution for the [BM⁴Py]⁺ cation with different anions, the selectivity S_{12}^∞ for separating aliphatic and aromatic hydrocarbons takes the following order: [BF₄]⁻ > [NTf₂]⁻ > [TOS]⁻, and the capacity k_2^∞ values follow the order (at $T = 328.15$ K) [NTf₂]⁻ > [BF₄]⁻ > [TOS]⁻.[8,16]

The phase diagrams of pyridinium-based ILs with water was investigated for [BM⁴Py][TOS][12] and for *N*-propyl-3-methylpyridinium bis{(trifluoromethyl)sulfonyl}imide, [PM³Py][NTf₂],[17] over a wide range of temperatures. The solubility of tosylate-based IL [BM⁴Py][TOS][12] in water reflects a simple eutectic mixture; the bis{(trifluoromethyl)sulfonyl}imide-based IL revealed the immiscibility in the liquid phase.[17] The solubility of a few other pyridinium-based ILs in water at temperature $T = 296.6$ K and the 1-octanol−water partition coefficient have also been reported in the literature.[18]
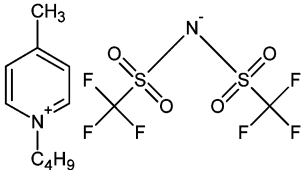
* To whom the correspondence should be addressed. E-mail: ula@ch.pw.edu.pl.
† Warsaw University of Technology.
‡ University of KwaZulu-Natal.
§ Visitor at Warsaw University of Technology, Poland.

TABLE 1: Investigated IL: Chemical Structure, Name, Abbreviation, and Measured Thermophysical Properties: Molar Volume ($V_{m,1}$) at $T = 298.15$ K, Temperature and Enthalpy of Fusion ($T_{fus,1}$ and $\Delta_{fus}H_1$, Respectively), Glass Transition Temperature ($T_{g,1}$), and Heat Capacity Change at $T_{g,1}$ ($\Delta C_{p(g),1}$)

structure	name
	N-butyl-4-methylpyridinium bis{(trifluoromethyl)sulfonyl}imide

	abbreviation	$\dfrac{M}{(\text{g·mol}^{-1})}$	$\dfrac{V_{m,1}(298.15)}{(\text{cm}^3\text{·mol}^{-1})}$
	[BM^{4}Py][NTf$_2$]	430.39	304.8

$\dfrac{T_{fus,1}}{(\text{K})}$	$\dfrac{\Delta_{fus}H_1}{(\text{kJ·mol}^{-1})}$	$\dfrac{T_{1(g)}}{(\text{K})}$	$\dfrac{\Delta C_{p(g),1}}{(\text{J·mol}^{-1})}$
291.4	21.94	195.9 (g)	149

The solubility of pyridinium-based ILs in alcohols depends mainly on the anion of the IL: [BM^{4}Py][TOS] and [BM^{3}Py]-[TOS] systems show simple eutectic mixtures with complete miscibility in the liquid phase;[11–13] [BM^{3}Py][NTf$_2$] and several pyridinium-based ILs (37) together with [BM^{3}Py][BF$_4$][15,19] all show LLE with upper critical solution temperatures (UCSTs).

The heats of mixing have been investigated for binary systems of pyridinium-based ILs with water and alcohols.[19,20] The heat capacities of pyridinium-based ILs were also measured.[21–23]

One of the aims of the present work is to study the influence of the asymmetry of the cation on the phase behavior of pyridinium bis{(trifluoromethyl)sulfonyl}imide ILs. The question is: how does the position of methyl group on the pyridinium ring ([BM^{3}Py]$^+$ vs [BM^{4}Py]$^+$) influence the binary phase diagrams? The investigation also includes the effect on solubility of: (1) the alkyl chain length of an alcohol; (2) the effect of the alkyl chain length of *n*-alkanes; (3) the alkyl chain length of substituent on the benzene ring; (4) the type of anion with the same cation; (5) and the type of cation linked to a bis{(trifluoromethyl)sulfonyl}imide anion.

Experimental Procedures and Results

Materials. [BM^{4}Py][NTf$_2$] has a purity of >0.999 mass fraction and was purchased from Liquids Technologies (Iolitec GmbH& Co. KG, Denzlingen, Germany). This IL is liquid at 298.15 K. The IL was further purified by subjecting the liquid to a very low pressure of about 5×10^{-3} Pa at a temperature about 280 K for approximately 5 h. This procedure removed any volatile chemicals and water from the IL. The structure of the investigated IL and the different physicochemical properties are presented in Table 1.

Water for the solubility measurements was twice distilled, degassed, deionized, and filtered with Milipore Elix 3. The alcohols used in phase equilibria measurements were purchased from Sigma Aldrich Chemie GmbH (Steinheim, Germany). All of the alcohols (except 1-dodecanol, which was used without further purification) were fractionally distilled to achieve a mass percent purity (checked by using gas chromatography) of >99.8% and then stored over a freshly activated molecular sieve (type 4A from Union Carbide). The purity in mass fraction and supplier of each of the other chemicals were as follows: benzene (CAS No. 71-43-2, Sigma-Aldrich, >99.97%); toluene (CAS No. 108-88-3, Fluka, >99.7%); ethylbenzene (CAS No. 100-41-4, Sigma-Aldrich, 99%); *n*-propylbenzene (CAS No. 103-65-1, Sigma-Aldrich, 98%); *n*-hexane (CAS No. 110-54-3, Merck, 99%); *n*-heptane (CAS No. 142-82-5, Sigma-Aldrich, 99%); *n*-octane (CAS No. 111-65-9, Sigma-Aldrich, 99%); and cyclohexane (CAS No. 110-82-7, Sigma-Aldrich, 99%).

Differential Scanning Microcalorimetry (DSC). The temperature of fusion ($T_{fus,1}$), enthalpy of fusion ($\Delta_{fus}H_1$), glass

transition temperature ($T_{g,1}$), and change of heat capacity at the glass transition temperature, $T_{g,1}$ ($\Delta C_{p(g),1}$), have been measured using a DSC technique. The applied scan rate was 5 K·min^{-1}, with a power and recorder sensitivity of 16 mJ·s^{-1} and 5 mV, respectively. The apparatus (Thermal Analysis Q200, USA with a liquid nitrogen cooling system) was calibrated with a 0.999999 mole fraction purity indium sample. The average value of the melting temperature was ($T_{fus,1} \pm 0.1$) K (average over three scans). The repeatability of that value was ±0.1 K. The enthalpy of fusion was ($\Delta_{fus}H_1 \pm 0.1$) kJ·mol^{-1}, and that of heat capacity at the glass transition temperature was ($\Delta C_{p(g),1} \pm 3$) J·mol^{-1}·K^{-1}. The thermophysical properties are shown in Table 1 and GRS 1S in the Supporting Information (SI).

Water Content. The water content was analyzed by a Karl Fischer titration technique (method TitroLine KF). The sample of IL was dissolved in methanol and titrated with steps of 2.5 μL. The results obtained have shown the water content to be less than 260 ppm. The error on the water content was ±10 ppm for the 3 mL injected IL.

Solid−Liquid and Liquid−Liquid Phase Equilibria Apparatus and Measurements. Solid solubilities or the disappearance of two phases observed with an increasing temperature have been determined using a dynamic (synthetic) method described previously.[3,11–13] The compound was kept under nitrogen in a dry box. Mixtures of solute and solvent were prepared by weighing the pure components to within 1×10^{-4} g. The sample of solute and solvent was heated very slowly (at less than 2 K·h^{-1} near the equilibrium temperature) with continuous stirring inside a Pyrex glass cell, placed in a thermostat. The crystal disappearance temperatures, or foggy solution disappearance detected visually, were measured with a calibrated Gallenkamp Autotherm II thermometer. The measurements were carried out over a wide range of solute mole fractions ranging from 0 to 1. The uncertainty of temperature

TABLE 2: Solid−Liquid Equilibria (SLE) and Liquid−Liquid Equilibria (LLE) of the Binary System {[BM^{4}Py][NTf$_2$] (1) + Water (2)}

x_1	T^{SLE}/K	T^{LLE}/K	x_1	T^{SLE}/K	T^{LLE}/K
1.0000	291.4		0.5929		341.9
0.9439	289.5		0.5552		346.5
0.8969	288.5		0.5369	287.3	
0.8468	287.4		0.5196		350.9
0.8261		297.5	0.4566		358.9
0.8051		305.0	0.4185	287.3	
0.7910	287.3	310.0	0.2948	287.3	
0.7547		316.8	0.0004		359.4
0.7152		323.1	0.0003		345.2
0.6702		331.0	0.0002		333.6
0.6428	287.3		0.0000	273.2	
0.6361		335.5			

Pyridinium-Based IL Solutions

J. Phys. Chem. B, Vol. 114, No. 46, 2010 **15013**

TABLE 3: SLE and LLE of the Binary System {[BM⁴Py][NTf₂] (1) + Solvent (2)}

x_1	T^{SLE}/K	T^{LLE}/K	x_1	T^{SLE}/K	T^{LLE}/K	x_1	T^{SLE}/K	T^{LLE}/K	x_1	T^{SLE}/K	T^{LLE}/K
1-Butanol											
1.0000	291.4		0.6622	281.6		0.3784	278.1	279.1	0.1137		291.7
0.9533	288.7		0.6175	280.4		0.3334	278.1	282.5	0.0785		291.7
0.9182	287.8		0.5778	279.5		0.2914		285.6	0.0678	278.1	
0.8804	286.8		0.5383	279.1		0.2509		288.1	0.0500		290.7
0.8424	285.7		0.4991	278.6		0.2286	278.1		0.0317		287.1
0.8003	284.7		0.4588	278.4		0.2047		290.1	0.0177		280.5
0.7452	283.6		0.4166	278.2		0.1523		291.2			
0.7054	282.5					0.1494	278.1				
1-Hexanol											
1.0000	291.4		0.6758	282.5		0.4283		312.6	0.1638		322.5
0.9737	289.1		0.6481		286.2	0.3958	282.5		0.1198		322.3
0.9203	287.5		0.6297	282.5	290.0	0.3773		316.5	0.0806		321.6
0.8753	286.1		0.5889		295.4	0.3377		318.6	0.0441		318.5
0.8344	285.3		0.5520		300.8	0.3187	282.5		0.0258		312.1
0.8042	284.8		0.5179		304.7	0.2950		320.7	0.0132		302.4
0.7804	284.0		0.4681	282.5		0.2562		321.7	0.0021		293.1
0.7437	283.2		0.4661		309.6	0.2081		322.4			
0.7077	283.0					0.1782	282.5				
1-Octanol											
1.0000	291.4		0.7977	285.9	296.1	0.4792	285.6	339.0	0.0779		345.5
0.9737	288.9		0.7607		304.3	0.4259		342.8	0.0402		339.8
0.9506	288.3		0.7230		311.7	0.3884		346.0	0.0175		334.3
0.9047	287.6		0.6825		317.9	0.3550		347.6	0.0091		324.5
0.8714	286.7		0.6514		322.8	0.3113		348.2	0.0050		313.1
0.8232	286.1		0.6123		327.2	0.2744	285.6	348.9	0.0042		285.6
0.8193		291.0	0.5694	285.6	331.9	0.2293		348.9	0.0000		259.2
0.8107		293.1	0.5192		336.3	0.1747		348.7			
0.7997		295.5				0.1258		347.8			
1-Decanol											
1.0000	291.4		0.8570		310.1	0.8031	287.9	326.4	0.4983		287.9
0.9756	289.8		0.8479		313.4	0.7874		331.7	0.2393		287.9
0.9316	288.7		0.8433	287.9		0.7740		334.3	0.0070		345.4
0.9076		290.3	0.8335		315.8	0.7605		336.5	0.0046		330.9
0.8911		296.4	0.8249		319.4	0.7480		338.2	0.0018		309.1
0.8885	287.9		0.8154		322.1	0.7256		342.0	0.0000		280.5
0.8781		303.0	0.8084		323.8	0.6876		349.0			
0.8667		307.3				0.6158	287.9				
Benzene											
1.0000	291.4		0.4360	259.7		0.2445	270.3		0.1544		297.3
0.9455	289.1		0.4121	257.2		0.2353	271.5		0.1532		303.5
0.9004	287.4		0.3936	255.0		0.2259	272.7		0.1521		312.4
0.8577	285.8		0.3743	252.1		0.2170	273.9		0.1510		318.3
0.8180	284.4		0.3581	250.3		0.2090	274.6		0.1500		323.8
0.7812	282.8		0.3429	253.1		0.2011	275.4		0.1488		329.5
0.7468	281.3		0.3296	255.2		0.1946	275.9		0.1477		338.7
0.7166	279.9		0.3180	257.9		0.1880	276.5		0.1467		344.9
0.6756	277.8		0.3071	259.9		0.1820	277.0		0.1351		278.7
0.6276	275.2		0.2965	261.6		0.1764	277.3		0.1142		278.7
0.5853	271.9		0.2864	263.8		0.1673	277.8		0.0977		278.7
0.5430	269.4		0.2757	265.4		0.1602	278.3		0.0643		278.7
0.5144	267.1		0.2673	266.6		0.1578	278.4	285.4	0.0000		278.3
0.4867	265.1		0.2587	268.1		0.1566		289.3			
0.4623	262.6		0.2517	269.5		0.1555		292.2			
Toluene											
1.0000	291.4		0.7083	280.5		0.4829	267.4		0.1983		299.8
0.9400	288.8		0.6752	278.8		0.4534	264.8		0.1973		289.2
0.8825	287.0		0.6377	277.1		0.4246	261.8		0.1962		276.6
0.8344	285.5		0.5813	274.2		0.4100	260.4		0.1954		268.3
0.7897	283.8		0.5496	272.5		0.3857	257.8		0.1941		253.5
0.7494	282.1		0.5146	269.8		0.3665	255.7				
Ethylbenzene											
1.0000	291.4		0.6862	279.4		0.4175	263.9		0.2779		288.4
0.9645	289.9		0.6525	277.8		0.3921	261.8		0.2758		283.4
0.9315	288.8		0.6034	275.5		0.3655	259.5		0.2739		279.8
0.8980	287.9		0.5587	273.3		0.3455	257.7		0.2720		276.4
0.8675	286.8		0.5247	271.3		0.3286	256.3		0.2702		272.0
0.8390	285.7		0.4954	269.4		0.2860		317.6	0.2683		267.4
0.8139	285.1		0.4695	267.6		0.2842		309.4	0.2664		263.5
0.7660	283.2		0.4462	265.9		0.2821		303.0	0.2638		257.4
0.7235	281.1					0.2800		295.7			

TABLE 3: Continued

x_1	T^{SLE}/K	T^{LLE}/K	x_1	T^{SLE}/K	T^{LLE}/K	x_1	T^{SLE}/K	T^{LLE}/K	x_1	T^{SLE}/K	T^{LLE}/K
					Propylbenzene						
1.0000	291.4		0.7066	281.0		0.4763	270.9		0.3514	264.9	285.5
0.9685	290.1		0.6763	279.9		0.4439	269.9		0.3478		279.8
0.9442	289.1		0.6509	278.8		0.4221	268.8		0.3444		275.4
0.9186	288.3		0.6261	277.7		0.4014	268.0		0.3410		270.6
0.8877	287.4		0.5938	276.3		0.3882	267.3		0.3376	264.0	265.1
0.8464	286.3		0.5641	274.9		0.3742	266.6		0.3071	264.0	
0.8065	285.0		0.5385	273.9		0.3623	265.9	303.2	0.2453	264.0	
0.7695	283.9		0.5040	272.2		0.3589		298.1	0.1789	264.0	
0.7370	282.2					0.3550		291.9			
					n-Hexane						
1.0000	291.4		0.9101	287.9		0.8771	287.9		0.8414		329.2
0.9819	289.6		0.9044	287.9		0.8727		300.2	0.8326		338.5
0.9759	289.4		0.8817	287.9		0.8702	287.9		0.8266		347.0
0.9447	288.9		0.8812		294.2	0.8602		311.3			
0.9276	288.5					0.8511		321.6			
					n-Heptane						
1.0000	291.4		0.9466	288.4		0.9154	288.4	304.0	0.8765	288.4	337.8
0.9804	289.5		0.9300	288.4	292.3	0.9004	288.4	314.8	0.8666	288.4	346.0
0.9632	288.8					0.8867	288.4	327.2			
					n-Octane						
1.0000	291.4		0.9548	288.8		0.9374	288.8	312.8	0.9151	288.8	347.6
0.9831	289.7		0.9413	288.8	302.7	0.9282	288.8	327.8	0.9039	288.8	
0.9687	289.0					0.9238	288.8	336.7			
					Cyclohexane						
1.0000	291.4		0.8834	287.4		0.7962	286.7	311.9	0.7238	286.7	340.8
0.9692	289.7		0.8599	286.9		0.7770	286.7	321.0	0.7099	286.7	346.6
0.9402	288.8		0.8364	286.7		0.7587	286.7	327.9	0.6938	286.7	353.0
0.9116	287.8		0.8163	286.7	300.5	0.7413	286.7	334.6			

measurements was ±0.05 K, and that of the mole fraction did not exceed ±0.0005. The reproducibility of the SLE/LLE experimental points was ±0.1 K. The experimental results are listed in Tables 2 and 3.

Results and Discussion

The basic thermal properties of the IL [BM⁴Py][NTf₂] are as follows: the enthalpy of fusion was ($\Delta_{fus}H_1 = 21.94$ kJ·mol⁻¹), and the melting temperature was $T_{fus,1} = 291.4$ K, which was much lower than that observed for [BM⁴Py][TOS].[12] The enthalpy of fusion determined in this work is higher than that of [BM⁴Py][TOS].[12]

The experimental data (temperature vs mole fraction of the IL) for the binary system with water and other solvents are presented in Figures 1 to 5. The liquidus curves for [BM⁴Py]-[NTf₂] are very short because the miscibility gap in the system with water (see Figure 1), alcohols, 1-octanol and 1-decanol

(see Figure 2), aromatic hydrocarbons (see Figure 3), aliphatic hydrocarbons (see Figure 4), and with cyclohexane (see Figure 5) is from the high mole fraction of the IL to the very low mole fraction of the IL. Slightly better solubility is observed for 1-butanol and 1-hexanol in the IL. The solubility of aromatic hydrocarbons in the IL is high, and the immiscibility gap started from mole fraction $x_1 = 0.3$ for *n*-propylbenzene (see Figure 3). The eutectic point for {[BM⁴Py][NTf₂] (1) + benzene (2)} is: $x_{1,e} = 0.358 \pm 0.002$, T_e/K = 250.3 ± 0.5. For the other mixtures with aromatic solvents, the eutectic point is shifted to the very low mole fraction of the solvent, because the melting temperatures of the toluene (178.15 K), ethylbenzene (179.15 K), and *n*-propylbenzene (173.15 K) are much lower than those for benzene (278.65 K). Thus, the phase diagrams of these three systems are different than this for {IL + benzene}. The interaction of the IL and aromatic solvents is quite high, because the solubility of the IL in benzene, toluene, and ethylbenzene
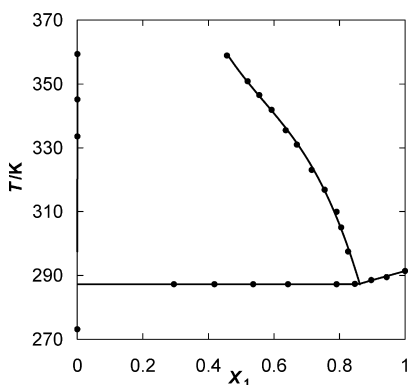

Figure 1. Plot of the experimental and calculated SLE and LLE of the {[BM⁴Py][NTf₂] (1) + water (2)} binary system. Lines have been calculated using the nonrandom two-liquid (NRTL) equation.
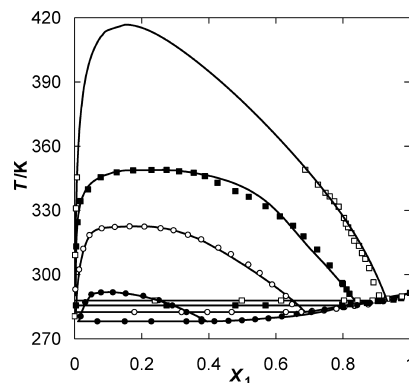

Figure 2. Plot of the experimental and calculated SLE and LLE of {[BM⁴Py][NTf₂] (1) + 1-alcohol (2)} binary systems: ●, 1-butanol; ○, 1-hexanol; ■, 1-octanol; □, 1-decanol. Lines have been calculated using the NRTL equation.
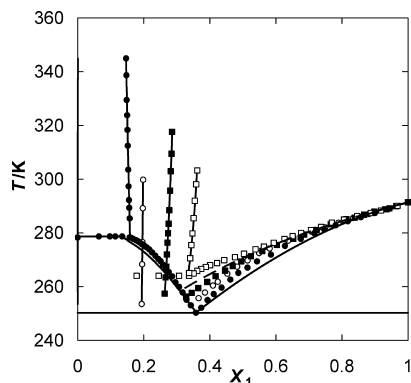
Pyridinium-Based IL Solutions

J. Phys. Chem. B, Vol. 114, No. 46, 2010 **15015**

Figure 3. Plot of the experimental and calculated SLE and LLE of {[BM^{4}Py][NTf$_2$] (1) + aromatic hydrocarbon (2)} binary systems: ●, benzene; ○, toluene; ■, ethylbenzene; □, propylbenzene. The dotted line represents the ideal solubility; solid lines have been calculated using the NRTL equation.
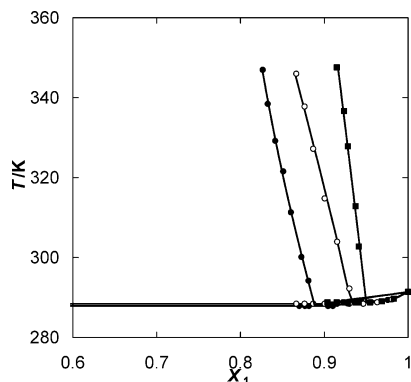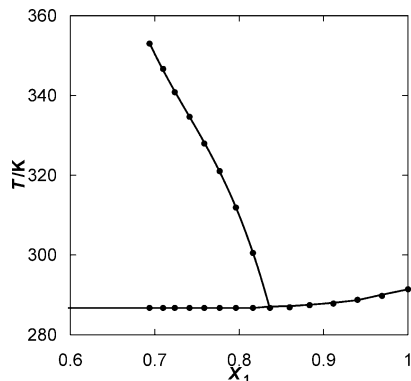

Figure 4. Plot of the experimental and calculated SLE and LLE of {[BM^{4}Py][NTf$_2$] (1) + aliphatic hydrocarbon (2)} binary systems: ●, *n*-hexane; ○, *n*-heptane; ■, *n*-octane. Lines have been calculated using the NRTL equation.

Figure 5. Plot of the experimental and calculated SLE and LLE of the {[BM^{4}Py][NTf$_2$] (1) + cyclohexane (2)} binary system. Lines have been calculated using the NRTL equation.

is higher than the ideal solubility. Only the solubility in *n*-propylbenzene is lower than the ideal solubility (see the dotted line in Figure 3). The liquid−liquid envelope (at IL-rich side) for the systems of alkylbenzenes seems to have a slightly positive slope at the investigated temperatures. It was observed by us in the previous work for different thiocyanate-based ILs.[3] Unfortunately, it is difficult to say if it can turn into a negative slope at higher temperatures and create the UCSTs. Maybe it can be observed for the solvents with high boiling temperatures.

On the basis of the phase diagrams the following trends can be observed: for all systems, a eutectic point was observed with immiscibility in the liquid phase; the solubility of the IL in
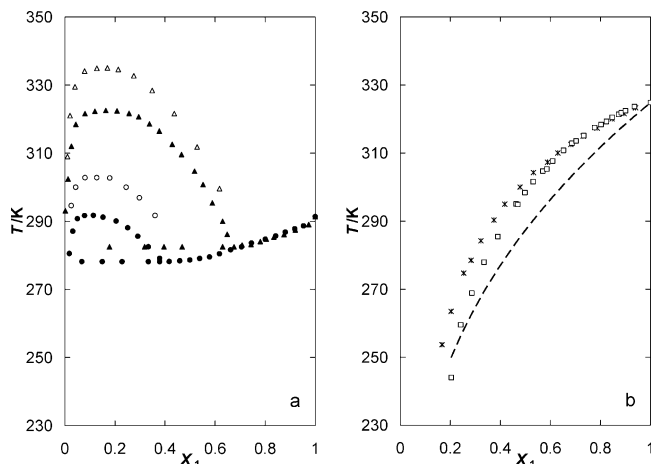

Figure 6. Plot of the experimental SLE and LLE of {[BM^{4}Py][NTf$_2$] (1) + 1-alcohol (2)} binary systems: (a) ●, {[BM^{4}Py][NTf$_2$] (1) + 1-butanol (2)}; ▲, {[BM^{4}Py][NTf$_2$] (1) + 1-hexanol (2)}; ○, {[BM^{3}Py][NTf$_2$] (1) + 1-butanol (2)};[15] △, {[BM^{3}Py][NTf$_2$] (1) + 1-hexanol (2)};[15] (b) □, {[BM^{4}Py][TOS] (1) + 1-butanol (2)};[12] ×, {[BM^{4}Py][TOS] (1) + 1-hexanol (2)};[12] dotted line represents the ideal solubility.

alcohols decreases as the length of carbon chain of an alcohol increases; and for alcohols and alkylbenzenes, the eutectic temperatures were expected far below 260 K and at a very low mole fraction of the IL.

The comparison of phase diagrams for the binary systems of {IL (1) + 1-butanol or 1-hexanol (2)} for ILs with the same anion [NTf$_2$]$^-$ but different cations, [BM^{3}Py]$^+$,[15] and for two cations, [BM^{4}Py]$^+$ and [BM^{3}Py]$^+$, but the tosylate anion is presented as an example in Figure 6 parts a and b, respectively. The UCST of the miscibility gap is higher for the IL with the [BM^{3}Py]$^+$[15] cation in comparison with [BM^{4}Py]$^+$ with the same anion [NTf$_2$]$^-$ (see Figure 6a). Replacing the anion [NTf$_2$]$^-$ with [TOS]$^-$[12] increases the solubility, and complete miscibility in the liquid phase is observed (see Figure 6b). The solubility of the tosylate-based ILs in 1-hexanol is lower than the ideal solubility (see Figure 6b). The same effect is observed for water.

Analyzing the possible use of [BM^{4}Py][NTf$_2$] for the separation of the aliphatics from aromatics, the discussion of the solubility of *n*-alkanes and benzene or alkylbenzenes in the IL has to be made. The solubility of *n*-alkanes in this work is comparable with the solubility of *n*-alkanes in [BM^{4}Py][TOS].[12] We can observe, however, huge differences in the solubilities of aromatic hydrocarbons in these two ILs. As is presented in Figure 7a and b, the solubility of benzene and propylbenzene is much higher in [BM^{4}Py][NTf$_2$] than in [BM^{4}Py][TOS]. After all, the working temperatures have to be 40 K higher for the tosylate-based IL. The conclusion can be made that [BM^4-Py][NTf$_2$] is more useful for the separation of aliphatic hydrocarbons from aromatic hydrocarbons. This information was first determined by the measurements of the activity coefficient at infinite dilution of different solvents in these two ILs. The selectivity at infinite dilution of the separation of hexane and benzene at $T = 328.15$ K was 9.5 and 17.3 for [BM^{4}Py][TOS][24] and [BM^{4}Py][NTf$_2$],[10] respectively. Similarly, the selectivity at infinite dilution of the separation of cyclohexane and benzene at $T = 328.15$ K was 4.9 and 9.9 for [BM^{4}Py][TOS][24] and [BM^{4}Py][NTf$_2$],[10] respectively. In conclusion, we can state that the [BM^{4}Py][NTf$_2$] IL reveals the average values of the selectivity for these separation problems in comparison with different pyridinium-based ILs.[5−9] However, the highest values of the selectivity in these two separation problems was observed for the *N*-butyl-
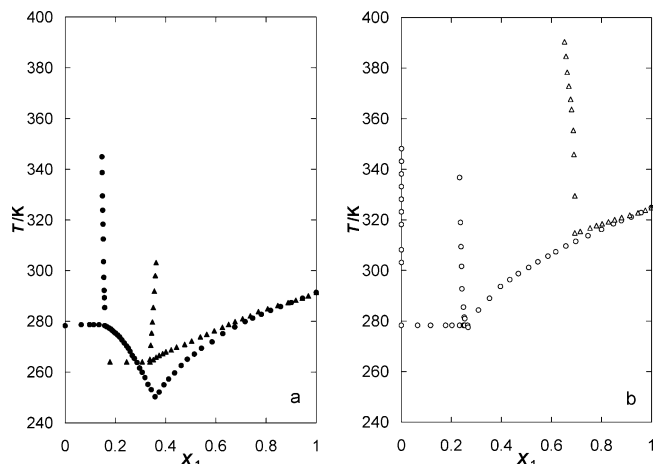
Figure 7. Plot of the experimental SLE and LLE binary systems of: (a) ●, {[BM⁴Py][NTf₂] (1) + benzene (2)}; ▲, {[BM⁴Py][NTf₂] (1) + n-propylobenzene (2); (b) ○, {[BM⁴Py][TOS] (1) + benzene (2)};[12] △, {[BM⁴Py][TOS] (1) + n-propylbenzene (2)}.[12]

4-methylpyridinium thiocyanate IL or 1-butyl-1-methylpyrrolidinium thiocyanate IL.[25] The values of selectivity of these two ILs for the n-heptane/benzene separation problem were 66.4 and 73.0, respectively, at the temperature $T = 323.15$ K.[25]

Modeling

Liquid−Liquid Phase Equilibrium Correlation. In this study, the NRTL model[26] was used to correlate the LLE phase equilibria. The adjustable parameters $(g_{12} - g_{22})$ and $(g_{21} - g_{11})$ of the model were found by minimizing the objective function OF:

$$OF = \sum_{i=1}^{n} [(\Delta x_1)_i^2 + (\Delta x_1^*)_i^2] \qquad (1)$$

where n is the number of experimental points, x is a mole fraction in the IL-rich phase, x^* is the IL-poor phase, and Δx is defined as

$$\Delta x = x_{calc} - x_{exp} \qquad (2)$$

The root-mean-square deviation of the mole fraction was defined as:

$$\sigma_x = \left(\sum_{i=1}^{n} \frac{(\Delta x_1)_i^2}{n-2} + \sum_{i=1}^{n} \frac{(\Delta x_1^*)_i^2}{n-2} \right)^{1/2} \qquad (3)$$

In this calculation, the parameter α_{12} is a constant of proportionality similar to the nonrandomness constant of the NRTL equation ($\alpha_{12} = \alpha_{21} = 0.1$ or 0.2) and was taken into account by choosing the value that gave the lowest deviation. The calculated values of the NRTL parameters and the corresponding root-mean-square deviations are presented in Table 4. The average deviation is in the range $\sigma_x = 0.0026$.

As we have mentioned already, for some mixtures under study, the solubility in the solvent-rich phase was impossible to detect by the visual method. These data were detected previously for some mixtures involving [BM⁴Py][TOS] from UV−vis spectra.[12] The values found were $x_1 = 7 \times 10^{-5}$ for benzene and $x_1 = 1 \times 10^{-5}$ for alkylbenzenes, n-alkanes, and cyclohexane.[12] It was assumed that the solubility in the dilute IL region for the system, measured in this work, was of the same order of magnitude. The results of the correlations are plotted in Figures 1 to 5.

Solid−Liquid Phase Equilibria Prediction. Since the solid−solid phase transition was not observed for [BM⁴Py]-[NTf₂], and the change of heat capacity at the melting temperature was not measured, a simplified general thermodynamic equation relating temperature, T^{SLE}, and the mole fraction of the IL, x_1, in all solvents has been fitted with the same parameters obtained from the correlation of LLE experimental data according to the equation:[27]

$$-\ln x_1 = \frac{\Delta_{fus}H_1}{R}\left(\frac{1}{T^{SLE}} - \frac{1}{T_{fus,1}} \right) + \ln \gamma_1 \qquad (4)$$

where $T_{fus,1}$, $\Delta_{fus}H_1$, T^{SLE}, x_1, and γ_1 refer to the melting temperature for the pure IL, the enthalpy of fusion for the pure IL, the SLE temperature, the equilibrium mole fraction, and the activity coefficient of the IL in the saturated solution, respectively. The first two values are given in Table 1, and the experimental data are listed in Tables 2 and 3. The enthalpy of melting is assumed

TABLE 4: Correlation of the SLE and LLE Data by Means of the NRTL Equation,ᵃ the Mole Fraction Deviations σ_x for the LLE, and the Temperature Deviations for the SLE

	$g_{12} - g_{22}$/J·mol⁻¹			$g_{21} - g_{11}$/J·mol⁻¹					
solvent	a_{12}	b_{12}	c_{12}	a_{21}	b_{21}	c_{21}	α	σ_x	σ_T/K
water	−92066	648.9	−1.197	233443	−1409	2.427	0.1	0.0018	0.19
1-butanol	50219	−211.8		−26184	170.0		0.1	0.0025	0.27
1-hexanol	18106	−85.17		19040	4.058		0.1	0.0059	0.98
1-octanol	94559	−547.9	0.774	−336248	2234	−3.555	0.2	0.0139	1.39
1-decanol	20570	−62.24		8933	17.51		0.2	0.0055	0.62
benzene	927.4	−35.23		7077	70.47		0.1	0.0002	1.84
toluene	−754.7	−25.58		−5668	119.2		0.2	0.0001	
ethylbenzene	−2496	−13.28		−4817	108.1		0.2	0.0003	
propylbenzene	−1453	−40.00		−22042	205.5		0.1	0.0005	
n-hexane	7135	−14.28		4418	72.02		0.2	0.0005	0.62
n-heptane	9702	−19.49		1775	79.35		0.2	0.0008	1.62
n-octane	7474	−30.47		−5161	118.6		0.1	0.0004	1.36
cyclohexane	15650	−68.34		13151	68.63		0.1	0.0018	0.76

ᵃ Parameters: $g_{12} - g_{22} = a_{12} + b_{12}T + c_{12}T^2$; $g_{21} - g_{11} = a_{21} + b_{21}T + c_{21}T^2$.

Pyridinium-Based IL Solutions

J. Phys. Chem. B, Vol. 114, No. 46, 2010 **15017**

TABLE 5: UCSTs Calculated by the NRTL Equation for the Binary System {[BM⁴Py][NTf₂] (1) + Solvent (2)}

binary mixture	x_1	T/K
1-butanol	0.1206	291.7
1-hexanol	0.1511	322.5
1-octanol	0.3305	348.9
1-decanol	0.1499	416.8
cyclohexane	0.0840	664.0

to be temperature-independent, whereas the activity coefficient is temperature, as well as solubility-dependent.

For the IL used in this work, the molar volume $V_{m,1} = 288.8$ cm³·g⁻¹(298.15 K), for the hypothetical subcooled liquid, was calculated by the group contribution method described by Barton.[28] The NRTL equation has two adjustable parameters P_1 and P_2 (the α parameter is fixed, additionally), which are determined by minimization of the objective function OF(P_1, P_2), defined as follows:

$$OF(P_1, P_2) = \sum_{i=1}^{n} [T_{exp,i} - T_{calc,i}(x_i, P_1, P_2)]^2 \quad (5)$$

where n denotes the number of experimental points. The Marquardt algorithm for solving nonlinear least-squares problems was successfully used in this work. As a measure of the reliability of the correlations, the root-mean-square deviation of temperature, σ_T, has been calculated according to the following definition:

$$\sigma_T = \left\{ \sum_{i=1}^{n} \frac{(T_{exp,i} - T_{calc,i})^2}{n - 2} \right\}^{1/2} \quad (6)$$

The values of the NRTL parameters and the corresponding root-mean-square deviations of temperature, σ_T, are reported in Table 4, and the resulting curves are presented together with the experimental points in Figures 1 to 5.

The results obtained indicate that the equation used was appropriate in providing a reliable description of the SLE measured in this work (except three systems with aromatic compounds). The average value of the root-mean-square deviations of temperature, σ_T, was 0.96 K.

Using the NRTL parameters, it was possible to calculate some of the UCSTs of the binary systems, which are presented in Table 5. For water and further non-presented solvents, the calculated temperatures were too high to be believed.

Concluding Remarks

Phase equilibria data, including SLE and LLE, for binary mixtures of the IL [BM⁴Py][NTf₂] with water, 1-alcohols, benzene and alkylbenzenes, *n*-alkanes, and cyclohexane have been measured. The (solid + liquid) phase diagrams for all the systems studied here show an eutectic point and immiscibility in the liquid phase. The results were compared to analogous ILs with the same cation and/or anion. A comparison of phase diagrams indicates that an exchange of the cation, [BM⁴Py]⁺ for [BM³Py]⁺, changes the physicochemical properties and solubility of the IL in alcohols, increasing the UCST. This is largely due to the symmetry of the cation.

The SLE diagrams and the LLE for [BM⁴Py][NTf₂] were compared to tosylate-based ILs in binary solutions with 1-alcohols. The solubility of the IL increases for the tosylate-based IL.

Benzene and the alkylbenzenes showed a much higher solubility than water and alcohols. Each of the *n*-alkanes showed a slightly lower solubility for the longer chain length of an alkane. The solubility of cyclohexane in [BM⁴Py][NTf₂] was higher than those of *n*-alkanes.

The simultaneous description of the LLE and SLE data was carried out by means of the NRTL equation. The results of the correlation and prediction were acceptable for most of the data.

References and Notes

(1) Holbrey, J. D.; López-Martin, I.; Rothenberg, G.; Seddon, K. S.; Silvero, G.; Zheng, X. *Green Chem.* **2008**, *10*, 87–92.
(2) Gao, H.; Luo, M.; Xing, J.; Wu, Y.; Li, Y.; Li, W.; Liu, Q.; Liu, H. *Ind. Eng. Chem. Res.* **2008**, *47*, 8384–8388.
(3) Domańska, U.; Królikowski, M.; Ślesińska, K. *J. Chem. Thermodyn.* **2009**, *41*, 1303–1311.
(4) Arce, A.; Francisko, M.; Soto, A. *J. Chem. Thermodyn.* **2010**, *42*, 712–717.
(5) Kato, R.; Gmehling, J. *Fluid Phase Equilib.* **2004**, *226*, 37–44.
(6) Inoue, G.; Iwai, Y.; Yasutake, M.; Honda, K.; Arai, Y. *Fluid Phase Equilib.* **2007**, *251*, 17–23.
(7) Heintz, A.; Kulikov, D. V.; Verevkin, S. P. *J. Chem. Thermodyn.* **2002**, *34*, 1341–1347.
(8) Heintz, A.; Kulikov, D. V.; Verevkin, S. P. *J. Chem. Eng. Data* **2001**, *46*, 1526–1529.
(9) Shimoyama, Y.; Hirayama, T.; Iwai, Y. *J. Chem. Eng. Data* **2008**, *53*, 2106–2111.
(10) Domańska, U.; Marciniak, A. *J. Chem. Thermodyn.* **2009**, *41*, 1350–1355.
(11) Domańska, U.; Królikowski, M.; Paduszyński, K. *J. Chem. Thermodyn.* **2009**, *41*, 932–938.
(12) Domańska, U.; Królikowski, M.; Pobudkowska, A.; Letcher, T. M. *J. Chem. Eng. Data* **2009**, *54*, 1435–1441.
(13) Letcher, T. M.; Ramjugernath, D.; Tumba, K.; Królikowski, M.; Domańska, U. *Fluid Phase Equilib.* **2010**, *294*, 89–97.
(14) Reddy, P.; Letcher, T. M. Phase equilibrium studies on ionic liquid systems for industrial separation processes of complex organic mixtures. In *Thermodynamics, Solubility and Environmental Issues*; Letcher, T., Ed.; Elsevier: Oxford, 2007.
(15) Crosthwaite, M.; Muldoon, M. J.; Aki, S. N. V. K.; Maginn, E. J.; Brennecke, J. F. *J. Phys. Chem. B* **2006**, *110*, 9354–9361.
(16) Mutelet, F.; Jaubert, J.-N. *J. Chromatogr., A* **2006**, *1102*, 256–267.
(17) Freire, M. G.; Neves, C. M. S. S.; Carvalho, P. J.; Gardas, R. L.; Fernandes, A. M.; Marrucho, I. M.; Santos, L. M. N. B. F.; Coutinho, J. A. P. *J. Phys. Chem. B* **2007**, *111*, 13082–13089.
(18) Freire, M. G.; Ventura, S. P. M.; Santos, L. M. N. B. F.; Marrucho, I. M.; Coutinho, J. A. P. *Fluid Phase Equilib.* **2008**, *268*, 74–84.
(19) Ortega, J.; Vreekamp, R.; Marrero, E.; Penco, E. *J. Chem. Eng. Data* **2007**, *52*, 2269–2276.
(20) Ortega, J.; Vreekamp, R.; Penco, E.; Marrero, E. *J. Chem. Thermodyn.* **2008**, *40*, 1087–1094.
(21) Crosthwaite, M.; Muldoon, M. J.; Dixon, J.-N. K.; Anderson, J. K.; Brennecke, J. F. *J. Chem. Thermodyn.* **2005**, *37*, 559–568.
(22) Diedrichs, A.; Gmehling, J. *Fluid Phase Equilib.* **2006**, *244*, 68–77.
(23) García-Miaja, G.; Troncoso, J.; Romaní, L. *J. Chem. Thermodyn.* **2009**, *41*, 161–166.
(24) Letcher, T. M.; Ramjugernath, D.; Królikowski, M.; Laskowska, M.; Naido, P.; Domańska, U. *Fluid Phase Equilib.* **2009**, *276*, 31–36.
(25) Domańska, U.; Królikowska, M. *J. Phys. Chem. B* **2010**, *114*, 8460–8466.
(26) Renon, H.; Prausnitz, J. M. *AIChE J.* **1968**, *14*, 135–144.
(27) Prausnitz, J. M.; Lichtenthaler, R. N.; Azevedo, E. G. *Molecular thermodynamics of fluid-phase equilibria*, 2nd ed.; Prentice-Hall Inc.: Engelwood Cliffs, NJ, 1986.
(28) Barton, A. F. M. *CRC Handbook of Solubility Parameters*; CRC Press: Boca Raton, FL, 1985; p 64.

JP105825C